A New Two-Port Network Model based Pilot Protection for AC Transmission Lines

S. M. Liu, *Member, IEEE*, L. L. Zhang, *Member, IEEE*, C. S. Fu and L. Jiang, *Member, IEEE*

***Abstract*-- Conventional pilot protections used for EHV/UHV AC transmission lines require data synchronization between the two terminals of transmission line and their performance is affected by the line capacitive charging current and load conditions. To tackle these problems, this paper proposes a new pilot protection scheme based on two-port network model of AC transmission lines. The new protection scheme calculates the two-port network parameters from the online measurements via sequence components method, then compares the solved parameters with their setting values to distinguish the internal and external faults. It does not require the data synchronization between two terminals of transmission line. Moreover, its performance is not affected by the line capacitive charging current and load conditions. The applicability of the proposed scheme for series compensated lines are also analyzed. Effectiveness and accuracy of the proposed protection scheme have been verified by simulation tests.**

***Index Terms*-- Pilot protection, transmission line, sequence components theory, two-port network, transmission network parameters**

I. Introduction

PILOT protections have been widely used for EHV/UHV transmission lines due to their merits of absolute selectivity and high speed [1]. There are two main types of pilot protections, unit type schemes and non-unit type schemes. The unit schemes, such as phase comparison schemes and current differential schemes [2,3], need to compare measurements from the two terminals of the transmission line to determine the tripping signal. The non-unit schemes, such as directional comparison scheme [4] and distance scheme [5], don't need to compare measurements from the two terminals and only require the transmission of logic signals from the two terminals, but they have very complex logic because of the requirements of dealing with power swing, inversion conditions, etc.

Current differential protection has been one of the most used unit-type pilot protection for EHV/UHV AC transmission lines, because of their simplicity and high reliability, and the development and the reduced cost of fiber-optic communication technology [6-9]. One special requirement of the current differential protection is that the current measurements of two terminals should be synchronized for the calculation of the differential current. To satisfy this requirement, algorithms such as "ping-pong" algorithm and the GPS based synchronized algorithm are proposed. The "ping-pong" algorithm uses four-time stamps gathered in a round-trip communication exchange, just as NTP protocol [10]. However, this algorithm requires a symmetrical communication channel, which means the length of Tx path should be equal to that of Rx path, and thus it is not suitable for an optical fiber network. Although the synchronized measurement based on GPS has high applicability and reliability [11], the receiving and processing of the satellite signal significantly increases the cost and application difficulty.

Another drawback of the unit protection schemes is that their sensitivity is seriously affected by the line capacitive charging current generated from distributed capacitor of long-distance transmission lines, during the normal state and external fault conditions. Compensation methods have been proposed to tackle this problem [12-14]. However, as capacitive current is calculated based on the steady-state, they cannot deal with the transient capacitive current which is much larger than the steady-state one. On the other hand, impedance-based pilot protection methods have been proposed to remove the capacitive current compensation [15-21], such as integrated impedance [15,16], fault voltage and current based integrated impedance to eliminate the effect of load current [17-20]. It should point out these impedance-based protections still require the data synchronization. Pilot differential protection based on virtual impedance of fault component is not affected by data synchronization [21], but the calculation of virtual impedance is very complex under the widely used series or parallel compensation on EHV/UHV transmission lines.

This paper investigates a new pilot protection principle based on the two-port network model (TPNM) of transmission line. The structure and parameters of the TPNM of a transmission line is only determined by the structure and the parameters of the line, and independent of system operating conditions and external components, thus the TPNM parameters can be chosen as the protection setting values. Under fault condition, by finding two groups of voltage and current values of the two-port network, the transmission line

This work was supported by the National Natural Science Foundation of China under Grant 51677108.

S. M. Liu and C. S. Fu are with Key Laboratory of Power System Intelligent Dispatch and Control of Ministry of Education, Shandong University, Jinan 250061, Shandong Province, China (e-mail: lsm@sdu.edu.cn).

L. L. Zhang is with School of Electric Power Engineering, South China University of Technology, Guangzhou 510640, Guangdong, China (e-mail: epzhangll@scut.edu.cn).

L. Jiang is with the Department of Electrical Engineering and Electronics, University of Liverpool, Liverpool, U.K. (e-mail: ljiang@liv.ac.uk).

TPNM parameters can be solved. By comparing the solved values with those setting ones, the protection can determine whether the fault is inside the transmission line or not. The proposed protection is not affected by the transmission line distributed capacitive current, and can be easily used on series compensated and parallel compensated transmission line, because these factors can be easily considered into the transmission line TPNM parameters due to the two-port network theory. Furthermore, because only amplitudes of the two-port network parameters are used, the proposed protection doesn't require the data synchronization.

The rest of the paper is arranged as follows. Section II introduces the basic principle of two-port network model and the characteristics of two-port network parameters. Section III presents the principle of the proposed protection scheme. The effectiveness of the proposed protection scheme is verified in Section IV via digital simulation tests based on a 1000 kV UHV transmission line model. Conclusions are given in Section V.

II. Two-Port Network Model

Based on the principle of sequence component analysis, a three-phase-transposed EHV/UHV transmission line can be modelled by three independent sequence circuits, which can be represented by two-port networks. Under the normal symmetrical operation condition, a transmission line has only the positive-sequence component and the relationship between voltage and current phasors of the two terminals could be expressed as [22]:

$$\begin{bmatrix} \dot{V}_{\mathrm{S}} \\ \dot{I}_{\mathrm{S}} \end{bmatrix} = \begin{bmatrix} A & B \\ C & D \end{bmatrix} \cdot \begin{bmatrix} \dot{V}_{\mathrm{R}} \\ -\dot{I}_{\mathrm{R}} \end{bmatrix} = T \cdot \begin{bmatrix} \dot{V}_{\mathrm{R}} \\ -\dot{I}_{\mathrm{R}} \end{bmatrix} \tag{1}$$

where subscripts S and R denote the Sending and Receiving terminals, respectively. A, B, C and D are components of the transmission matrix T, representing the open-circuit reverse voltage gain, the negative short-circuit transfer impedance, the open-circuit transfer admittance, and the negative short-circuit reverse current gain, respectively. The unit of B is Ohm, the unit of C is Siemens, while A and D have no unit.

When an internal fault occurs on the transmission line, a new branch will be added inside the two-port network, which divides the original circuit into two parts, the left part and the right part shown in Fig. 1. According to the transmission matrix cascade computing principle, the transmission matrix becomes:

$$T_{\mathrm{fault}} = \begin{bmatrix} A_{\mathrm{fault}} & B_{\mathrm{fault}} \\ C_{\mathrm{fault}} & D_{\mathrm{fault}} \end{bmatrix} = T_{\mathrm{left}} \cdot \begin{bmatrix} 1 & 0 \\ \dfrac{1}{R_{\mathrm{f}}} & 1 \end{bmatrix} \cdot T_{\mathrm{right}} \tag{2}$$

where the subscript 'fault' denotes the corresponding variable is the one under fault condition. And T_{left} and T_{right} are the transmission matrices of the left part network and the right part network, respectively, and they have the relationship with the original transmission matrix of sound line as [22]:

$$T = T_{\mathrm{left}} \cdot T_{\mathrm{right}} \tag{3}$$

From the two-port network theory, it could be known that the parameters of the matrix T only depend on the structure and parameters of the circuit inside the two-port network. They will change due to an internal fault while keep just the same when an external fault occurs or system operation condition changes.

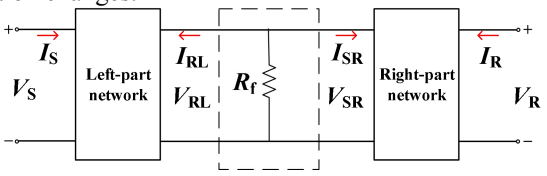

Fig. 1 A two-port network model of a transmission line with internal fault.

Therefore, a new protection scheme can be proposed to identify internal fault on transmission line by monitoring the changes in the parameters of the matrix T.

III. Two-Port Network Model Based Protection Scheme

The values of the parameters of matrix T, under normal operation conditions, can be calculated according to the electrical parameters of the transmission line, these values are chosen as setting values in TPNM protection.

The matrix T of a short or middle-length transmission line could be deduced from its lumped parameter π-type equivalent circuit [23] as:

$$T = \begin{bmatrix} \dfrac{Z \cdot Y}{2} + 1 & Z \\ Y \cdot \left(1 + \dfrac{Z \cdot Y}{4}\right) & \dfrac{Z \cdot Y}{2} + 1 \end{bmatrix} \tag{4}$$

where Z is the total series impedance, and Y is the total shunt admittance.

For a long-length transmission line, the matrix T could be deduced from uniform transmission line equation as:

$$T = \begin{bmatrix} \mathrm{ch}\gamma l & Z_0 \mathrm{sh}\gamma l \\ \dfrac{1}{Z_0} \mathrm{sh}\gamma l & \mathrm{ch}\gamma l \end{bmatrix} \tag{5}$$

where Z_0 is the characteristic impedance, γ is the propagation constant, and l is the length of the transmission line.

When a fault is detected, the parameter values of T_{fault} can be calculated by solving (1) with on-line measured voltage and current phasors. If the solved values are obviously different from the setting values, an internal fault can be confirmed. Based on this principle, this paper proposes a new protection scheme called Two-Port Network Model Protection (TPNM Protection).

Note that there are four parameters (A, B, C and D) in the matrix T, but there are only two equations in (1). To solve out all parameters, another two equations are needed. By employing the method of symmetrical components and superposition theorem, the following four group measurements can be obtained:

1) Negative sequence voltages and currents measured after fault;
2) Superimposed positive sequence voltages and currents;
3) Positive sequence voltages and currents measured after the fault;
4) Positive sequence voltages and currents measured before fault (load voltages and currents).

Any two groups of upper four group of measurements can be used to solve the matrix T parameters. For example, if the positive- and negative-sequence components are used, the following equation can be derived from (1):

$$\begin{bmatrix} |A| & |B| \\ |C| & |D| \end{bmatrix} = \begin{bmatrix} V_{S1} & V_{S2} \\ I_{S1} & I_{S2} \end{bmatrix} \cdot \begin{bmatrix} V_{R1} & V_{R2} \\ -I_{R1} & -I_{R2} \end{bmatrix}^{-1} \tag{6}$$

where subscripts 1 and 2 denote positive- and negative-sequence, respectively. $|A|$, $|B|$, $|C|$ and $|D|$ means only magnitudes of the four parameters are solved, because only the magnitudes of voltages and currents are used in (6). This makes the TPNM protection has the merit of no synchronization need for the voltage and current measurement of the two terminals of the transmission line.

All four parameters of the matrix T can be used to design the protection scheme. To simplify the proposed TPNM protection, only $|C|$ is chosen, the reason is as follow. Series compensation is widely used in EHV/UHV transmission lines. It can be proved that $|A|$, $|B|$ are affected by the operational status of the series compensators, while $|C|$ and $|D|$ are completely not affected. The theoretical proof is not presented due to space limit, and the simulation verification is given in Section IV.F. Compared with $|D|$, $|C|$ has the advantages of being less affected by the load, thus $|C|$ is chosen as the protection criterion. Therefore, the TPNM protection employ the following criterion to identify an internal fault on the transmission line:

$$\left| |C| - |C_{\text{set}}| \right| > \varepsilon_C \tag{7}$$

where the subscript 'set' denotes the setting value of matrix T, ε_C is the threshold related to measurement error and calculation error and chosen as following for enough safety and sensitivity:

$$\varepsilon_C = 0.4|C_{\text{set}}| \tag{8}$$

The flowchart shown in Fig. 2 describes the implementation steps of the TPNM protection. Firstly, the positive and negative sequence components of voltages and currents are calculated and compared with threshold values, which are 0.02 U_N and 0.1I_N respectively, where subscript N denote rated values.

If the negative sequence components are large enough, which means the fault is an asymmetrical one, the negative sequence components and the superimposed positive-sequence components are used to calculate $|C|$. Otherwise, the fault is a symmetrical one, the positive sequence components after and before the inception of fault are used to calculate $|C|$.

The calculated $|C|$ is then substituted into (7). If the criterion of (7) is satisfied, an internal fault is identified. Afterwards, the protection relay will conduct phase selection and trip the faulted phase(s). If the criterion is not satisfied, the protection will go back to the first step and repeat all the procedures again.

IV. Case Study

The proposed TPNM protection is verified based on simulation studies of a Chinese ultra-high voltage (UHV) pilot project [24], as shown in Fig. 3. The 1000 kV 654 km transmission line transmits electric power from Jindongnan substation in Shanxi Province to Jingmen substation in Hubei Province. The line is divided into two parts by Nanyang switching station. The Jindongnan to Nanyang part (J-N line) is 363 km and the Nanyang to Jingmen part (N-J line) is 291 km. The sending end (Jindongnan side) and receiving end (Jingmen side) power systems are represented as two 500 kV Thevenin

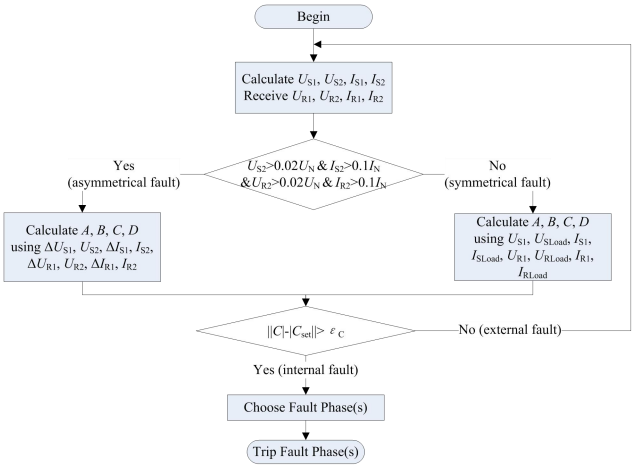

Fig. 2 The flowchart of the proposed TPNM protection scheme.

equivalent sources. The electrical parameters of the transmission line and the equivalent sources are shown in Appendix A. The proposed scheme is tested and compared with the traditional current differential protection (TCD protection).

The setting values of the matrix T can be calculated based on transmission line distributed model or lumped parameters model. For the UHV transmission lines, distributed model in (5) is used to as:

$$\begin{bmatrix} |A_{\text{set}}| & |B_{\text{set}}| \\ |C_{\text{set}}| & |D_{\text{set}}| \end{bmatrix} = \begin{bmatrix} 9.25E-01 & 9.33E+01 \\ 1.55E-04 & 9.25E-01 \end{bmatrix} \tag{9}$$

where the subscript 'set' denotes the setting value

Although only $|C|$ is used in the TPNM protection criterion, all four parameters of matrix T are calculated and illustrated in the following analysis for better understanding of the scheme.

A. Influence of Distributed Capacitive Current

For EHV/UHV transmission lines, the distributed capacitive current is significant and has adverse effect on TCD protection. In contrast, because the capacitance of the distributed capacitor has been included in the calculation of matrix T parameters, such as the distributed model in (5) or the lumped parameter model in (4), distributed capacitive current will not affect the criterion of the TPNM protection.

Taking the 1000 kV pilot project as an example, if there is no shunt reactance compensation, the magnitude of the capacitive current in J-N line can be as large as 1318 A under normal operation condition. The pilot project is designed to have 2800 MW rated transmission capacity, which means the rated current of the transmission line is 1800 A. The capacitive current will consume 73.22% rated current which will significantly reduce the power transfer capability of the UHV transmission line. Therefore, there are four shunt reactors

installed at the two terminals of each line, as illustrated in Fig. 3. The reactance of 4 reactors are shown in Table V.

Because the transmission line ought to be under-compensated, even with shunt reactance compensation, there will still be 162.67A capacitive current in J-N line under normal operation situation. According to the suggestion of a commercial TCD protection relay produced by Beijing Sifang automation Co., Ltd. China [25], the threshold should be not smaller than 2.5 times of the capacitive current, i.e. 406.68 A.

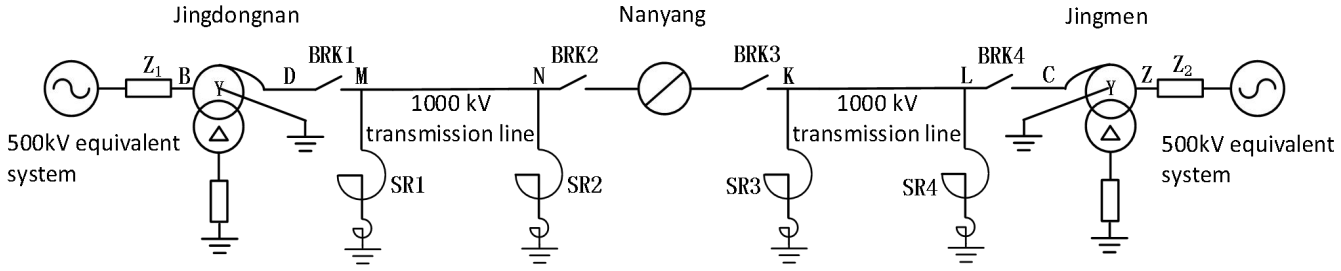

Fig. 3. Model of an ultra-high voltage transmission line installed in China.

TABLE I
Short Circuit Resistance of Line-to-Ground Fault that Current Different Protection Can React

Distance (km)	Resistance (Ω)	Distance (km)	Resistance (Ω)
0.0	79.82	217.8	119.86
36.3	85.76	254.1	127.95
72.6	91.93	290.4	136.50
108.9	98.33	326.7	145.53
145.2	105.10	363.0	154.82
181.5	112.28		

TABLE II
Errors Between On-line Transmission Network Parameters and Theoretical Parameters

Parameter	Maximum Value	Relative Error
$\|A\|$	9.8026e-01	0.0056%
$\|B\|$	9.3333e+01	0.0101%
$\|C\|$	2.2454e-04	0.3802%
$\|D\|$	9.9877e-01	0.9445%

With such a high threshold, the sensitivity of the TCD protection will be decreased sharply, especially for short circuit fault with high resistance. Table I shows the largest resistance of line-to-ground fault, occurring at different fault positions along the J-N line, that TCD protection can detect. In the table, the values in the first column are the distances between Jindongnan substation to different fault locations. From Table I it could be seen that, due to capacitive current, the TCD protection cannot meet the requirement that relay should be able to detect single-line-to-ground faults with transient resistance up to 600 Ω for UHV transmission lines, some special measurement should be taken [8].

As for the TPNM protection, the shunt reactors will influence the setting values of matrix T parameters. This effect can be taken into account very easily, by using cascade computing principle:

$$\begin{bmatrix} |A_{set}| & |B_{set}| \\ |C_{set}| & |D_{set}| \end{bmatrix} = \begin{bmatrix} 9.80E-01 & 9.33E+01 \\ 2.24E-04 & 9.99E-01 \end{bmatrix} \quad (10)$$

By simulating all kinds of asymmetrical external faults, at different positions of N-J line with various short circuit resistances, the errors between on-line calculated transmission network parameters and the setting values can be obtained and are listed in Table II. The results show that the relative errors are very small, which means the distributed capacitive current has no effect on TPNM protection. With threshold setting as mentioned in (8), the TPNM protection can detect line-to-ground faults with fault resistance larger than 600 Ω, at any position along the transmission line.

TABLE III
Asynchronous Time Caused Pseudo-Differential Currents

Time (ms)	Current (A)	Time (ms)	Current (A)
0.1	242.00	-0.1	84.25
0.2	321.51	-0.2	22.10
0.3	401.04	-0.3	81.49
0.4	408.52	-0.4	159.83
0.5	559.91	-0.5	239.15
0.6	639.18	-0.6	318.65
0.7	718.31	-0.7	398.18
0.8	797.27	-0.8	477.67
0.9	876.04	-0.9	557.06
1.0	954.59	-1.0	636.34

B. Influence of Data Synchronization

The TCD protection needs synchronized sampling of currents measured at the two terminals of a transmission line. Asynchronous sampling will cause pseudo-differential currents, which may lead to mal-operation of TCD protection.

Table III shows the magnitude of pseudo-differential currents resulting from asynchronous sampling, under the rated operating condition. In the table, the positive time values mean the sampling of sending end is leading that of receiving end, while negative time values mean lagging. It can be seen that, with the threshold set to 406.68 A, an asynchronous time more than 0.4 ms leading or 0.8 ms lagging will result in incorrect operation of TCD protection.

As for the TPNM protection, as described in Section Ⅲ, by using only magnitude values of calculated parameter C, it does not be influenced by asynchronous sampling problem.

The above analysis is based on the steady-state components. The total fault current and voltage also have transient components, which include the decaying dc components and high frequency ones [1]. For UHV transmission line faults, the decaying dc currents will further deteriorate the operating

characteristics of the TCD protection further [8].

While by applying the DC filter presented in [26], TPNM protection will not be affected by the transient components. In order to confirm this statement, external line-to-ground faults were applied at the middle point of N-J line with 10 Ω transient resistance. In different test cases, the asynchronous time delay varies from -10.0 ms to +10.0 ms and the beginning time of data window varies from 0 ms to 100 ms after the fault inception. The calculated values of $|C|$ for all cases are illustrated in Fig. 4.

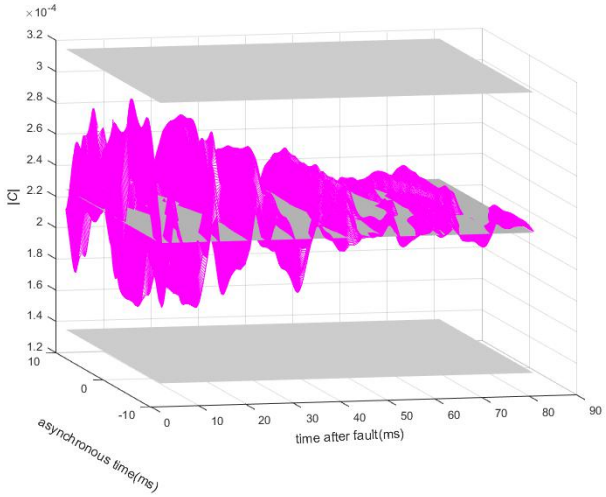

Fig. 4. The influence of synchronization in the calculation of the transmission network parameter $|C|$.

It can be seen that, considering the fault transient, the values of $|C|$ varies according to asynchronous time and beginning time of data window. Comparing with the setting value of $|C_{set}|$, 2.24e-04, the maximum relative error is 36.61%, which is obtained when the data window starts at 0 ms after fault inception and the asynchronous time is 6.0 ms leading. The maximum error is smaller than the security margin of 0.4 defined by (8). Moreover, if the data window starts at 50 ms after the fault inception, the value of $|C|$ does almost not been affected by the asynchronous time anymore, which verified that TPNM is immune to asynchronous problems in steady state.

C. Influence of High Transient Resistance Faults

The transient resistance detection capability of TPNM protection for internal single-line-to-ground faults on the J-N line is illustrated in Fig. 5. There are four subfigures in Fig. 5, illustrating the calculation results of $|A|$, $|B|$, $|C|$ and $|D|$ separately. In each subfigure, there are three horizontal planes, which are the lower bound plane, the setting value plane and the upper bound plane, respectively, in order from bottom to top. The bounds for $|C|$ are defined by (8) and (10). As $|A|$, $|B|$ and $|D|$ are less affected by the transient, the bounds for them are set as ±10% from the setting values. For $|C|$ and $|D|$, the three horizontal planes seem compressed into one plane, as the calculated parameters are far from the setting values.

It is worth pointing out that it can be seen from Fig. 5 that for faults at different positions, the curves of the four parameters are all parallel to the Y-axis, which means their values are independent of the fault resistance. The reason is analyzed in Appendix B.

D. Influence of Different Fault Types

In order to verify the performance of TPNM protection, different types of internal faults were also applied to the J-N line at different positions with the transient resistance varies from 0 to 50 Ω. Fig. 6 illustrates the results of phase-to-phase faults and Fig. 7 shows the results of three-phase short circuit faults. It could be seen that the results are very similar to that shown in Fig. 5. Therefore, for different fault types, TPNM also has very high sensitivity.

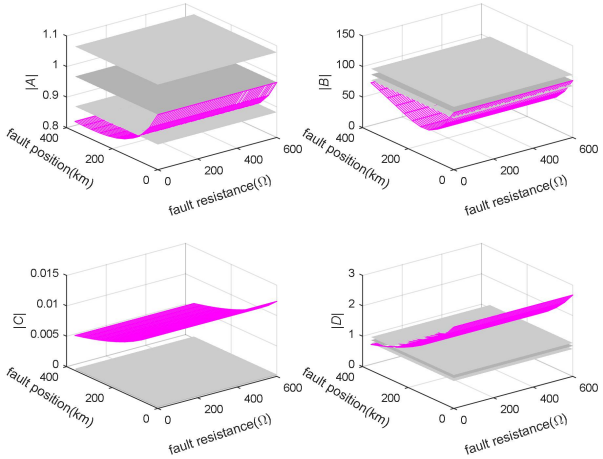

Fig. 5. The results of transmission network parameters under internal line-to-ground faults with transient resistance.

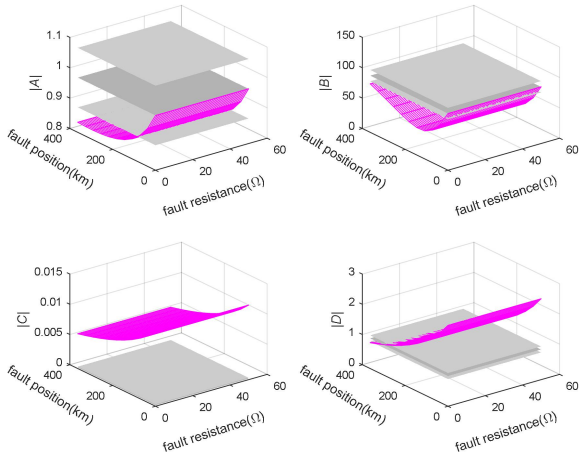

Fig. 6 The results of transmission network parameters under internal Phase B-to-Phase C faults with transient resistance.

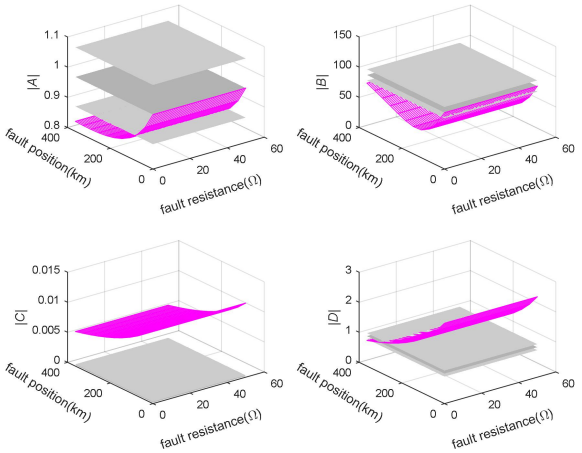

Fig. 7 The results of transmission network parameters under internal three-phase symmetrical faults with transient resistance.

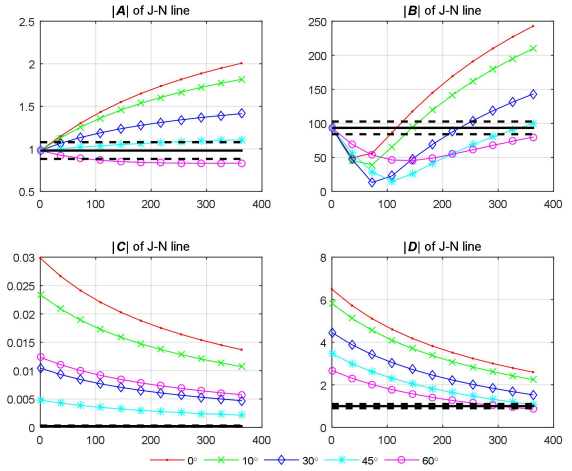

Fig. 8. The results of internal AN faults of Jindongnan-Nanyang line.

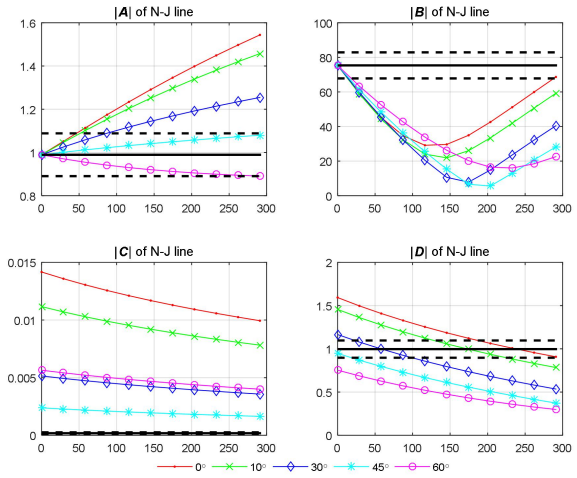

Fig. 9. The results of internal AN faults of Nanyang-Jinmen line.

E. Influence of Different System Conditions

The above given simulation results are all about Jindongnan-Nanyang transmission line, and the system potential angles are all 60° which represents heavy load condition. Simulation studies have also been conducted under other system conditions and the results are illustrated below.

Because the transmission network parameters of the simulation model are independent of fault resistance, the Y-axis of the figures will be ignored in the following simulation results. In each subfigure, there are three horizontal lines, the dash-dot line is the lower bound, the black line is the setting value, and the dashed line is the upper bound.

Fig. 8 shows simulation results of internal AN faults on Jindongnan-Nanyang transmission line, with fault position varies from 0 to 363 km. Each curve represents an individual system potential angle, varying from 0 to 60°. It shows that TPNM protection fits for all load conditions.

Fig. 9 shows the simulation results of internal AN faults on Nanyang-Jinmen transmission line, with fault position varies from 0 to 291 km. Each curve represents an individual system potential angle, from 0 to 60°. It shows that TPNM protection fits for different transmission lines.

TABLE IV
Transmission Network Parameters with Series Compensating Capacitors

Degree	C (μF)	$\|A\|$ (e-1)	$\|B\|$ (E+1)	$\|C\|$ (e-4)	$\|D\|$ (e-1)
20%	166.30	9.76	11.24	2.24	9.99
30%	110.86	9.74	12.20	2.24	9.99
40%	83.15	9.72	13.16	2.24	9.99
50%	66.52	9.70	14.11	2.24	9.99
60%	55.43	9.67	15.07	2.24	9.99

F. Influence of Series Compensation Lines

Series compensators are widely used for long distance high voltage transmission line to increase power transfer capability and improve power system stability. Although the pilot project UHV lines do not install series compensators, it is worth studying the suitability of TPNM protection for series compensated transmission lines.

One reason of the C parameter of the matrix T is chosen as criterion of the proposed protection scheme is that C is not affected by the series compensation of the transmission line. Although the pilot project doesn't install series compensation, tests are designed to verify the effectiveness of the TPNM under different operation status of the series compensation.

To simplify the analysis, a set of three-phase static capacitors are installed at the Jindongnan terminal of the J-N line in the simulation model, and a resistor is parallel-connected with the capacitors of each phase to simulate the effect of SSC protection circuit. Different values of resistance represent different operating situations of the protection circuit of the series compensator.

At first, an infinite resistance was used to simulate the normal state of the compensator. Changing the compensation level between 20%~60%, the matrix T parameters of J-N line are listed in Table IV, which shows that parameters $|C|$ and $|D|$ are not affected by the change of compensation level. The compensation level of 40% was used in the subsequent simulation studies.

Secondly, the resistance was set to different values to simulate different by-pass states of the protection circuit, in which a resistance of 0 Ω means that the capacitor are completely short-circuited.

For an external AN fault occurs on N-J line, Fig. 10 illustrates the results obtained with different values of parallel resistance and shows that the values of $|A|$ and $|B|$ change with the parallel resistance, while the values of $|C|$ and $|D|$ are not affected.

For an internal AN fault on J-N line, Fig. 11 illustrates the results obtained with different values of parallel resistance. As can be seen, the values of $|A|$, $|B|$ and $|D|$ are equal to their setting values under some conditions, while the values of $|C|$ keep far away from its upper bound. This has confirmed that the suitability of using $|C|$ as the criterion of the TPNM protection.

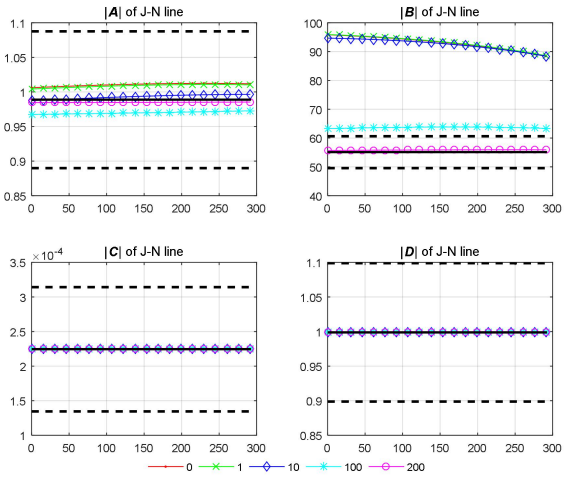

Fig. 10 The results of matrix T parameters under external line-to-ground faults with SSSC short circuit.

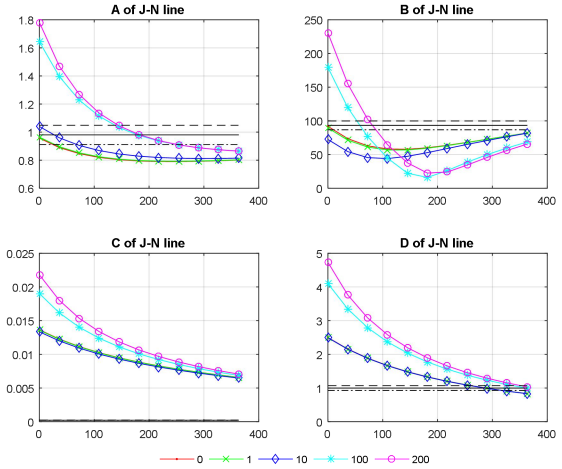

Fig. 11 The results of matrix T parameters under internal line-to-ground faults with SSSC short circuit.

V. Conclusion

This paper proposes a new pilot protection for AC transmission lines based on two-port network model (TPNM). As parameters of the two-port network model are determined only by the structure and electrical parameters of the transmission line, and are independent of the system operating conditions and the parameters of external components, the proposed new protection scheme is not affected by the distributed capacitive current and the fault transient resistance, and has a much higher sensitivity than the traditional current differential protection which performance is affected by the asynchronous sampling and distributed capacitive current. Furthermore, because only amplitudes of the two-port network parameters are used, the proposed protection doesn't require the data synchronization. The proposed scheme has been verified via numerical simulation based on a pilot 1000 kV UHV transmission line, and compared with the current differential protection.

VI. Appendix A Simulation Model Parameters

TABLE V
Parameters of 1000kV Transmission Line (per kilometer).

Symbol	Quantity	Value
r_{1_J}	Positive-sequence resistance (Ω) of J-N line	0.00758
l_{1_J}	Positive-sequence inductance (H) of J-N line	0.83922e-3
c_{1_J}	Positive-sequence capacitance (F) of J-N line	0.013970e-6
r_{0_J}	Zero-sequence resistance (Ω)of J-N line	0.15421
l_{0_J}	Zero -sequence inductance (H) of J-N line	2.6439e-3
c_{0_J}	Zero -sequence capacitance (F) of J-N line	0.009296e-6
r_{1_N}	Positive-sequence resistance (Ω)of N-J line	0.00801
l_{1_N}	Positive-sequence inductance (H) of N-J line	0.83747e-3
c_{1_N}	Positive-sequence capacitance (F) of N-J line	0.013830e-6
r_{0_N}	Zero-sequence resistance (Ω)of N-J line	0.15630
l_{0_N}	Zero -sequence inductance (H) of N-J line	2.4895e-3
c_{0_N}	Zero -sequence capacitance (F) of N-J line	0.008955e-6
X_{SR1}	Reactance of reactor 1 on J-N line (Ω)	1260
X_{SR2}	Reactance of reactor 2 on J-N line (Ω)	1680
X_{SR3}	Reactance of reactor 3 on N-J line (Ω)	1680
X_{SR4}	Reactance of reactor 4 on N-J line (Ω)	2016

TABLE VI
Parameters of Thevenin Equivalent Sources.

Parameter	Jindongnan 500-kV system (Sending end)	Jinmen 500-kV system (Receiving end)
Short-circuit level (min)	5189MVA	23148MVA
Short-circuit level (max)	28062MVA	30858MVA
X1_min	9.79ω	9.096ω
X1_max	52.81ω	11.85ω
X0_min	15.44ω	18.19ω
X0_max	64.79ω	23.15ω
Transformers Leakage inductance	18%	18%

VII. Appendix B Analyze of Fault Resistance Effect

Fig. 5 shows that the calculated transmission network parameters are independent of fault resistance. The reason is explained below.

From sequencing network analysis method, the negative sequence network of the transmission line with an internal fault can be illustrated as Fig. 12, in which, Z_S and Z_R are equivalent negative sequence impedances of the equivalent power sources at two terminals, and E_f is negative sequence source.

From fault component analysis method, the superimposing

positive sequence network of an internal fault transmission line can also be illustrated as Fig. 12, while Z_S, Z_R, E_f and Z_f represent the positive-sequence values.

From Fig. 12, we get:

$$\left.\begin{aligned} V_{RL} &= V_{SR} \\ I_{RL} &= k \cdot I_f \\ I_{SR} &= (1-k)\cdot I_f \end{aligned}\right\} \Rightarrow \begin{bmatrix} V_{RL} \\ I_{RL} \end{bmatrix} = \begin{bmatrix} 1 & 0 \\ 0 & \dfrac{1-k}{k} \end{bmatrix} \cdot \begin{bmatrix} V_{SR} \\ I_{SR} \end{bmatrix} \qquad (11)$$

where k is the branch coefficient of the circuit that at the right hand to the box in dashed line. From circuit theory, it is known that the proportion of ISR accounted for I_f only relates to the ratio between the impedance of the right-side circuit and the impedance of the left side circuit, but is unrelated to E_f and Z_f. That means k is independent of fault resistance.

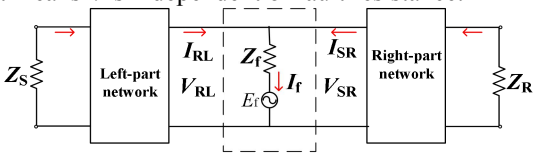

Fig. 12 The two-port network of fault-component equivalent circuit

As mentioned before, the positive sequence impedances of the left part network and the right part network are identical to those of negative sequence circuit. If only Z_S and Z_R of the positive sequence circuit are equal to those of negative sequence circuit, then the branch coefficient k will be the same for positive- and negative- sequence circuit.

Analogous to (2), the transmission matrix of Fig. 12 can be written in the form as below:

$$T_{fault} = \begin{bmatrix} A_{fault} & B_{fault} \\ C_{fault} & D_{fault} \end{bmatrix} = T_{left} \cdot \begin{bmatrix} 1 & 0 \\ 0 & \dfrac{1-k}{k} \end{bmatrix} \cdot T_{right} \qquad (12)$$

With k is independent of fault resistance and is identical for positive- and negative-sequence circuit, the transmission matrix of transmission line with internal fault, T_{fault}, is independent of fault resistance.

VIII. References

[1] P. M. Anderson, *Power System Protection*. New York: Wiley, 1998.

[2] Y. Z. Ge, A. D Wang and H. L. Tao, "Phase-comparison pilot relays using fault superimposed components," in *Proc. APSCOM*, 1991, Hong Kong, pp. 833-838.

[3] T. Sugiyama, T. Kano, M. Hatata and S. Azuma, "Development of a PCM Current Differential Relaying System Using Fiber-Optic Data Transmission," *IEEE Trans. Power App. Syst.*, vol. PAS-103, no. 1, pp. 152-159, Jan. 1984.

[4] Y. Y. Ma, G. B. Zou, Z. J. Gao and T. Du, "A fast directional comparison pilot protection for UHV transmission line," in *Proc. APPEEC*, 2016, Xi'an, pp. 526-530.

[5] E. L. Harder, B. E. Lenehan and S. L. Goldsborough, "A new high-speed distance-type carrier-pilot relay system," *Electr. Eng.*, vol. 57, no. 1, pp. 5-10, Jan. 1938.

[6] X. Lin, Z. Li, K. Wu and H. Weng, "Principles and Implementations of Hierarchical Region Defensive Systems of Power Grid," *IEEE Trans. Power Deliv.*, vol. 24, no. 1, pp. 30-37, Jan. 2009.

[7] X. Lin, Q. Tian and M. Zhao, "Comparative analysis on current percentage differential protections using a novel reliability evaluation criterion," in *IEEE Trans. Power Deliv.*, vol. 21, no. 1, pp. 66-72, Jan. 2006.

[8] Z. Y. Xu, Z. Q. Du, L. Ran, Y. K. Wu, Q. X. Yang and J. L. He, "A Current Differential Relay for a 1000-kV UHV Transmission Line," *IEEE Trans. Power Del.*, vol. 22, no. 3, pp. 1392-1399, July 2007.

[9] S. Dambhare, S. A. Soman and M. C. Chandorkar, "Adaptive Current Differential Protection Schemes for Transmission-Line Protection," *IEEE Trans. Power Deliv.*, vol. 24, no. 4, pp. 1832-1841, Oct. 2009.

[10] D. L. Mills. "Internet time synchronization: the network time protocol," *IEEE Trans. Commun.*, vol. 39, pp. 1482–1493, Oct 1991.

[11] A. G. Phadke, B. Pickett, M. Adamiak, et al, "Synchronized sampling and phasor measurements for relaying and control," in *IEEE Trans. Power Deliv.*, vol. 9, no. 1, pp. 442-452, Jan. 1994.

[12] T. S. Bi, Y. L. Yu, S. F. Huang and Q. X. Yang, "An accurate compensation method of distributed capacitance current in differential protection of UHV transmission line," in *Proc. IEEE PES General Meeting*, 2005, San Francisco, CA, 2005, pp. 770-774

[13] Y. Zhang, J. Suonan, "Phaselet-based current differential protection scheme based on transient capacitive current compensation," *IET Gener. Transm. Distrib.*, vol. 2, no. 4, pp. 469-477, July 2008.

[14] H. Ito, I. Shuto, H. Ayakawa, P. Beaumont and K. Okuno, "Development of an improved multifunction high speed operating current differential relay for transmission line protection," in *Seventh International Conference on Developments in Power System Protection (IEE)*, Amsterdam, Netherlands, 2001, pp. 511-514.

[15] J. Suonan, X. Deng and K. Liu, "Transmission line pilot protection principle based on integrated impedance," *IET Gener. Transm. Distrib.*, vol. 5, no. 10, pp. 1003-1010, October 2011.

[16] S. He, J. Suonan and Z. Q. Bo, "Integrated Impedance-Based Pilot Protection Scheme for the TCSC-Compensated EHV/UHV Transmission Lines," *IEEE Trans. Power Deliv.*, vol. 28, no. 2, pp. 835-844, April 2013.

[17] J. Suonan, K. Liu and G. Song, "A Novel UHV/EHV Transmission-Line Pilot Protection Based on Fault Component Integrated Impedance," *IEEE Trans. Power Deliv.*, vol. 26, no. 1, pp. 127-134, Jan. 2011.

[18] J. Xia, S. Jiale, X. Deng, L. Wang, S. He and K. Liu, "Enhanced transmission line pilot impedance and pilot protection," *IET Gener. Transm. Distrib.*, vol. 5, no. 12, pp. 1240-1249, December 2011.

[19] J. Xia, S. Jiale, G. Song, L. Wang, S. He, and K. Liu, "Transmission line individual phase impedance and related pilot protection" *Int. J. Electr. Power Energy Syst.*, vol. 33, no. 9, pp. 1563-1571.

[20] T. G. Bolandi, H. Seyedi, S. M. Hashemi and P. S. Nezhad, "Impedance-Differential Protection: A New Approach to Transmission-Line Pilot Protection," *IEEE Trans. Power Deliv.*, vol. 30, no. 6, pp. 2510-2518, Dec. 2015.

[21] J. Ma, X. Pei, W. Ma and Z. Wang, "A New Transmission Line Pilot Differential Protection Principle Using Virtual Impedance of Fault Component," *Can. J. Electr. Comp. Eng.*, vol. 38, no. 1, pp. 37-44, winter 2015.

[22] J. W. Nilsson, S. Riedel, *Electric Circuits*, 7th Edition, New Jersey: Pearson Prentice Hall, 2005

[23] J. J. Grainger, W. D. Stevenson, *Power system analysis*, New York: McGraw-Hill, 1994

[24] Z. Y. Liu, *Ultra-High Voltage AC/DC Grids*, Oxford: Elsevier Inc, 2015

[25] *Manual of CSC-213 optical fiber differential protection relay and measurement and control device*. Beijing Sifang Automation Co., LTD., Beijing, 2006

[26] Y. Cho, C. Lee, G. Jang and H. J. Lee, "An Innovative Decaying DC Component Estimation Algorithm for Digital Relaying," *IEEE Trans. Power Deliv.*, vol. 24, no. 1, pp. 73-78, Jan. 2009.